Journal of Engineering and Applied Sciences 13 (14): 5789-5795, 2018
ISSN: 1816-949X


# Corrosion Behaviour of Mild Steel in 0.5 M Sulphuric Acid Media in the Presence of Potassium Chromate

[1]Olugbenga Adeshola Omotosho, [1]Joshua Olusegun Okeniyi, [3]Jacob Olumuyiwa IKOTUN, [1,2]Cleophas Akintoye Loto and [2]Abimbola Patricia Idowu Popoola
[1]Department of Mechanical Engineering, Covenant University, 112001 Ota, Nigeria
[2]Department of Chemical and Metallurgical Engineering, Tshwane University of Technology, 0001 Pretoria, South Africa
[3]Department of Civil Engineering and Building, Vaal University of Technology, Vanderbijlpark 1900, South Africa

**Abstract:** This research investigates the behaviour of $K_2CrO_4$ on mild steel corrosion in 0.5 M $H_2SO_4$ at ambient temperature of 30°C. The study was conducted using weight loss and potentio-dynamic polarization measurements. Data were recorded from the weight loss tests while the readout from the potentiostat was documented. Adsorption studies were also carried out. Furthermore, an investigation was conducted using surface coverage against concentration plot to determine when the best surface would be obtained during the experiment. Results from the study revealed that inhibitor efficiency increased as inhibitor concentration increased. The potentio-dynamic polarization plot also identified the inhibition mechanism of action as mixed but predominantly anodic type inhibition with maximum $E_{corr}$ displacement of 68 mV. The adsorption of the inhibitor agrees with the Langmuir adsorption isotherm while the separation factor which is a component of the Langmuir expression showed a favourable adsorption. The Gibbs free energy of adsorption showed negative value (-9.8 kJ/mol) depicting a spontaneous process with a prevalence of physical adsorption. The first day curve showed the best surface coverage values across all inhibitor concentrations utilized.

**Key words:** Corrosion, weight loss, potentiodynamic polarization, Tafel slope, adsorption isotherm, physical adsorption

## INTRODUCTION

The problems associated with corrosion is often considered to be economical because of consequences like loss of man-hours, facility replacement costs, compensation litigation by polluted communities, implied costs resulting from corrosion monitoring, maintenance and rehabilitation (Okeniyi *et al*., 2012, 2014a, b; Omotosho *et al*., 2012, 2014). However, this is not the only concern because the effect of corrosion has a substantial influence on environmental safety. For example, the corrosion of sulphuric acid storage tanks and pipelines in the Motiva petrol refining facility in the US in 2001 led to the failure of the storage tanks and resulted in the death of one worker and injury to eight others. The surrounding water body was also contaminated leading to the loss of marine life. The report of the ultrasonic test revealed that continuous corrosion of the sulphuric acid tank was the reason for the failure because 50% of the corrosion allowance was lost in a sizeable portion of the exposed area of the tank.

The use of corrosion inhibitors has been identified as an effective corrosion control system (Finsgar and Jackson, 2014; Rani and Basu, 2012). However, it begins with understanding the mechanisms by which inhibitors are introduced into an aggressive acidic environment to stifle the reaction between the material and the environment (Onuchukwu, 1988). Normally, inhibition process is triggered by either the chemisorptions or physisorption route. In the physisorption route inhibitor molecules become bonded to the cathodic sites of the metal surface, essentially suppressing the metallic dissolution process. On other hand the chemisorbed route ensures the anodic site is sheltered to decrease the characteristic ionization of the metal (Oguzie *et al*., 2005). It would seem that chemisorbed molecules of efficient inhibitors are overtly biased towards the anodic sites as they find greater expression in the region by protecting it (Deberry *et al*., 1984).

Chromate inhibitors are known to have the tendency to stifle reaction at the anode (Okonji *et al*., 2015a-c). However, since, inhibitors are environment specific it is

**Corresponding Author:** Joshua Olusegun Okeniyi, Department of Mechanical Engineering, Covenant University, 112001 Ota, Nigeria

important to gain more insight into the behaviour of potassium chromate in the sulphuric acid media. The adsorption layer of chromates is primarily made up of chromate oxide and it functions as a barrier separating the metal from the aggressive acidic media. The extent to which the process proceeds will depend on the metal involved, inhibitor structure, concentration and environmental temperature. Therefore, this study deals with the corrosion inhibition behaviour of mild steel in 0.5 M $H_2SO_4$ solution in the absence and presence of potassium chromate. The investigation will be conducted by monitoring of the corrosion process with gravimetric (weight loss) and electrochemical techniques.

## MATERIALS AND METHODS

**Preparation of mild steel specimen and test solutions:** Mild steel sheet was cut into coupons measuring 2×2×0.3 cm for gravimetric measurements. For the linear sweep voltametry tests, the electrodes sizes had an exposure area 1 $cm^2$ with a long electrical wire connection for electrochemical contact to the Digi-Ivy potentiostat. The mild steel specimen utilized in this study was analyzed for its chemical composition in the Department of Metallurgical Engineering, University of Lagos, Nigeria and the metal was found to have the following composition (in wt.%): 0.2654% Mn, 0.1203% C, 0.008% P, 0.034% S, 0.2212% Ni and the rest Fe. The aggressive media was 0.5 M $H_2SO_4$. The stock concentration of the acid with a purity and density of 94% and 1.84 $g/cm^3$, respectively was obtained from Sigma Aldrich, USA. The 0.5 M acid concentration was obtained by diluting a stock concentration of the $H_2SO_4$ (18.1 M) with distilled water in a fume chamber until the desired concentration was attained. $K_2CrO_4$ with 99% purity was obtained from Burgoyne Burbidges and Co, (India). The potassium chromate inhibitor concentration was prepared by making up the diluted concentration of the chromate inhibitor and the acid to 1 liter in a flat bottom flask. The concentration of the inhibitor for both test technique was varied from 2-10 g/L with increments of 2 g/L.

**Gravimetric (weight loss) measurements:** The test coupons were chemically treated before the test according to ASTM D2688-94 R99 (2005) procedures. The coupon weights were recorded before the experiment. At the end of the tests, the samples were subject to post-experimental cleaning. This procedure was conducted in accordance with ASTM (2005). To obtain the weight loss data, the readings after the experiment were subtracted from the reading before the experiment. The specimens were then immersed in 0.5 M $H_2SO_4$ with and without the varying inhibitor concentrations for 60 days at ambient temperature of 30°C. The weight loss readings were taken every 4 days but the reading for the 1st day of the experiment was also taken. Before taking measurements every 4 days, the coupons were removed from the test solution, rinsed, dried well and weighed.

**Electrochemical tests:** The electrochemical technique of potentio-dynamic polarization (Tafel) was conducted using Digi-Ivy potentiostat instrument (Model DY 2312) purchased from the U.S. The test solution was introduced into a three-electrode electrochemical cell kit model K47 manufactured by Princeton Applied Research in the U.S. The exposed surface area of 1 $cm^2$ for mild steel sample was embedded in a resin epoxy system with wire connection linking it from the test solution in the corrosion cell kit to the instrument. Prior to commencement of the tests the working electrode was treated with chemicals according to procedures earlier stated. The working electrode was polished before use. Other electrodes in the corrosion cell kit were a Ag/AgCl electrode as the reference electrode and graphite rod as the counter electrode. A steady-state reading of open circuit potential by metal sample was reached by the working electrode before commencement of the experiment. Potentio-dynamic polarization monitoring at a scan rate of 100 mV/sec was conducted from an anodic potential and cathodic potential of +0.5 V and -1.0 V, respectively (Omotosho *et al*., 2017a, b, 2016a-c).

**Corrosion rate analyses:** The weight loss data from the gravimetric tests were used to calculate the corrosion rate, $CR_{gr}$, using the expression in Eq. 1 (Omotosho *et al*., 2011; Eddy *et al*., 2015; Umoren *et al*., 2007; Karthik and Sundaravadivelu, 2013):

$$CR_{gr}(mmpy) = \frac{87.6W_L}{A \times T \times D} \quad (1)$$

Where:
A = The Area ($cm^2$)
$W_L$ = Mass change (g)
T = The Time of immersion (hr)
D = The Density of mild steel ($g/cm^3$)

Also, the corrosion rate ($CR_{pl}$) from potentiodynamic polarization tests were obtained from machine readout using Eq. 2 (Omotosho *et al*., 2017a, b, 2016a-c; Canmet, 2008):

$$CR_{pl} = \frac{3.27 \times 10^{-3} \times i_{corr} \times EW}{D} \quad (2)$$

Where:
EW = The Equivalent Weight (g)
$i_{corr}$ = Corrosion current density ($\mu A/cm^2$)
D = Density ($g/cm^3$)

**Inhibitor efficiency:** Corrosion rate values from the gravimetric experiment is then used for estimating the Inhibition Efficiency (IE%) of the $K_2CrO_4$ inhibitor using Eq. 3 (Okeniyi *et al*., 2014a-d, 2015a-c, 2016a-d, 2017a-c; Yadav *et al*., 2010):

$$IE\% = \frac{CR_{unihibited\text{-}sample} - CR_{inhibited\text{-}sample}}{CR_{unihibited\text{-}sample}} \times 100 \quad (3)$$

Similarly, the surface coverage ($\theta$) was estimated using in Eq. 4 (Okeniyi *et al*., 2015a-d 2017a-c; Karthikaiselvi and Subhashini, 2014):

$$IE\% = \frac{CR_{unihibited\text{-}sample} - CR_{inhibited\text{-}sample}}{CR_{unihibited\text{-}sample}} \quad (4)$$

## RESULTS AND DISCUSSION

Figure 1 shows the graph of Corrosion Rate ($CR_{gr}$) against time for the mild steel sample immersed in $H_2SO_4$ in the presence of $K_2CrO4$ at ambient temperature of 30°C. The control sample displayed very high CR values at the beginning of the experiment (first 24 h). This value, however, kept reducing as the experiment progressed but the very high initial value of the control sample $CR_{gr}$ ensured that the average of the $CR_{gr}$ values of the control was the highest. Figure 1b is a rescaled plot to view the disparity in $CR_{gr}$ values from 20 days to the end of the experiment, since, the curves on the plot (Fig. 1a) for the entire experiment is not delineated. As the experiment progressed at some point the $CR_{gr}$ of the inhibited samples were higher than that of the control. The 2 g/L inhibitor concentration displayed higher $CR_{gr}$ values than the control on the 28 and 36th day of the experiment. Generally, the $CR_{gr}$ values of the inhibited samples were lower than the control throughout the test period. This implies that the inhibitor was effective in retarding corrosion of mild steel sample in the acid solution.

Figure 2 shows the inhibition efficiency of potassium chromate inhibition based on weight loss tests. The trend of the inhibition efficiency in increasing order is; 2<4<6<8<10 g/L. This simply means that the inhibitor efficiency increased as inhibitor concentration increased. This indicates that for this particular corrosion system more of the molecules cover a larger surface area with a passive film thereby stifling the corrosion process.

Figure 3 is a plot of the curves of surface coverage ($\mu$) against inhibitor concentration as the experiment progressed. It is obvious from the graph that the curve for the first day produced the best surface coverage, possibly because no activity had really started to hamper the film

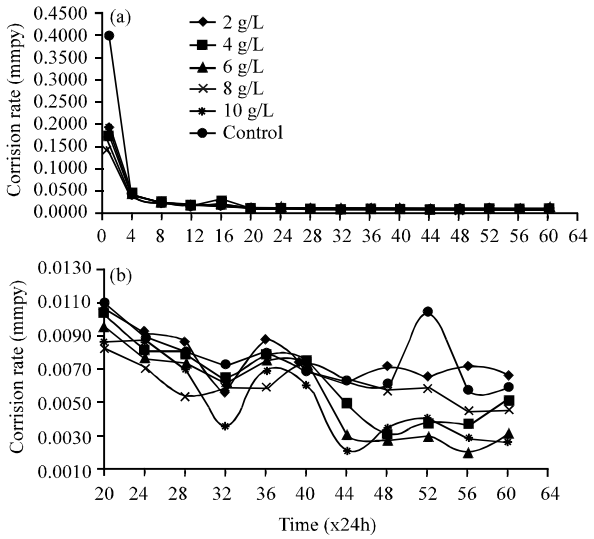


Fig. 1: Graph of corrosion rate against time for the immersion of mild steel samples in 0.5 M $H_2SO_4$ solution at ambient temperature of 30°C: a) Normal scale for 60 days and b) Rescaled to view 0.0010-0.0110 mmpy for 20-60 days

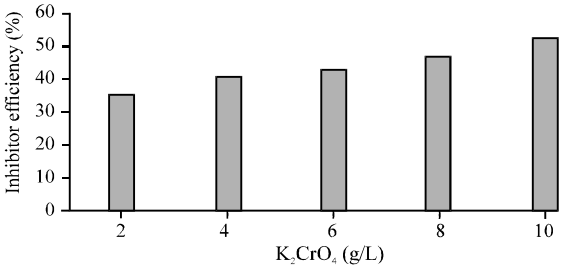


Fig. 2: Inhibition efficiency of potassium chromate on the corrosion of mild steel in 0.5 M $H_2SO_4$ solutions at ambient temperature of 30°C

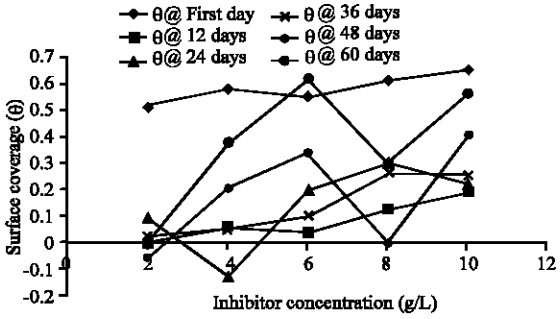


Fig. 3: Variation of surface coverage ($\mu$) with potassium chromate concentration (g/L) at a temperature of 30°C for different time intervals for mild steel immersed in 0.5 M $H_2SO_4$

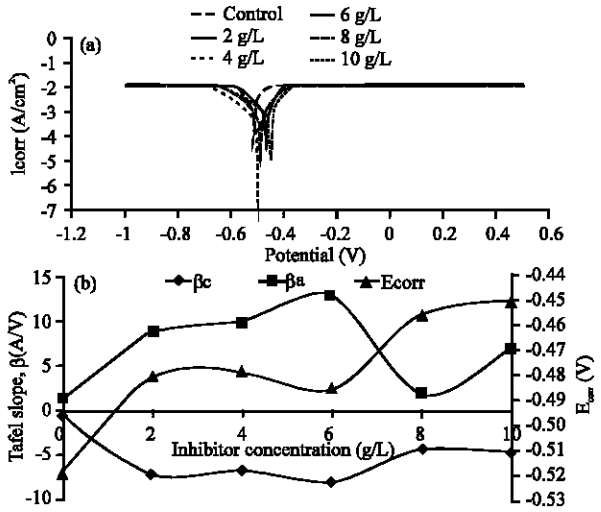


Fig. 4: Plots of kinetic parameters from electrochemical experiments: a) Potentio-dynamic polarization plots from LSV monitoring and b) Plots of corrosion potential and Tafel slopes against concentration of $K_2CrO_4$ from LSV experiments at ambient temperature of 30°C

forming process of the chromate inhibitor. The change in μ values for the first day at the lowest and highest concentration was very low but generally an uptrend was observed. From Fig. 3, the 60 days curve also showed high μ values at a concentration of 6 g/L, however, it showed a very low μ value at concentration of 2 g/L. The μ values of the 60 days curve fluctuated between 6-10 g/L concentration. In terms of its performance the 60 days curve was next to the first day curve. For the 24 and 48 days curve, the fluctuations of the curve were quite obvious and it occurred between the 6 and 10 g/L concentrations while the 12 and 36 days curve displayed slight fluctuations. Generally, all the curves showed an uptrend in μ values as concentration increased. However, the best time for the inhibitor to adhere to the metal sample surface is the first day.

Figure 4 shows the plot of the kinetic parameters of the electrochemical experiment. Figure 4a shows the graph of the Tafel plots of the control and inhibited samples. A look at the graph shows a clear shift towards the anodic direction of the curves of the inhibited samples. The curve for 10 g/L inhibitor concentration shifted most to the anodic direction. The average maximum displacement of the $E_{corr}$ value of the inhibited sample from the control is 68 mV suggesting that the $K_2CrO_4$ inhibitor acts as a mixed but predominantly anodic inhibitor. Earlier studies had established that $E_{corr}$ values <85 mV is mixed with anodic bias (Omotosho *et al*., 2016b). Anodic inhibitors act by stifling reactions at the anodic sites. Therefore, the inhibitor acted by reducing the anodic metal dissolution. Figure 4b is a plot of the Tafel constants and corrosion potential against concentration. The anodic and cathodic slope curves are clearly separated in the graph. The anodic curve displays an uptrend as the inhibitor concentration increases up till 6 g/L and thereafter decreases at 8 g/L and then increases again at 10 g/L concentration. This behaviour is similar to the behaviour of the surface coverage curves in Fig. 3 where the θ values also decreased and increased at same concentration. Thus, this shows an agreement in the relationship between these two graphs (Fig. 3 and 4b). Also, the value of $E_{corr}$ drifts from the cathodic region at the beginning when concentration is zero (control) into the anodic region of the graph and stays in the anodic region at the high concentration of 10g/L. It is also noted from Fig. 4b, that all inhibited samples displayed $E_{corr}$ values in the anodic region. This behaviour clearly agrees with the $E_{corr}$ displacements values that inferred an anodic inhibition mode.

Table 1: R-values of different adsorption isotherms employed for metal-$K_2CrO_4$ interaction mechanism in 0.5 M $H_2SO_4$

| Adsorption isotherm | R-values |
|---|---|
| Frumkin | 0.504 |
| Flory-Huggins | 0.766 |
| Boris-Swinkel | 0.840 |
| Temkin | 0.912 |
| Dubinin-Radushkevich | 0.920 |
| El-Awady | 0.920 |
| Freundlich | 0.930 |
| Langmuir | 0.969 |

**Adsorption studies:** Adsorption isotherms are normally deployed to describe the interaction mechanisms by the fitting of the test data to any of the adsorption isotherms identified for use. This experimental data fit was conducted using; Frumkin, Flory-Huggins, Boris-Swinkel, Temkin, Dubinin-Radushkevich, El-Awady, Freundlich and Langmuir isotherms. The results of the linear regression of the isotherms are shown in Table 1.

In Table 1, the R-values of each of the isotherms are exhibited and based on this Langmuir adsorption isotherm performed best. This was because it had the highest R-value. The expression shown in Eq. 5 (Foo and Hameed, 2010), represents the Langmuir adsorption equation, i.e:

$$\frac{C}{\theta} = \frac{1}{K_{Lg}Q_K} + \frac{C}{Q_K} \quad (5)$$

$K_{Lg}$ and $Q_K$ is the Langmuir isotherm constant and maximum monolayer capacity (mg/g). $K_{Lg}$ in the Langmuir

Table 2: Parameters of the linear regression of langmuir isotherm plot and separation factor

| Slope | Intercept | $Q_K$ | $K_{Lg}$ | $R_{Lg}$ | Favourability condition |
|---|---|---|---|---|---|
| 0.607 | 0.689 | 1.647 | 0.881 | 0.362 | Favourable |

expression is related to $R_{Lg}$ in the separation factor expression in Eq. 6 (Okeniyi, 2015a-c, 2016a-d; Omotosho *et al*., 2016; Foo *et al*., 2010):

$$R_{Lg} = \frac{1}{1+K_{Lg}C_i} \quad (6)$$

$R_{Lg}$ and $C_i$ are defined as the separation factor and the corrosion performance at the starting concentration, respectively.

By finding the logarithm of the Langmuir expression and thereafter plotting log (C/μ) versus log C, it was possible to determine the slope and intercept and compare the values from the graph to initial Langmuir expression. This comparison enables the deduction of the parameters shown in Table 2.

Inhibitors adsorption can be ranked based on the $R_{Lg}$ values which show the degree of favourability. Studies have shown that when $R_{Lg}$ values are greater than 0 and <1, the adsorption is favourable. Whereas when $R_{Lg}$ is more than 1 it is not favourable. On the other hand, when it is equivalent to 1, the adsorption is identified as linear while when it is zero, it is irreversible (Okeniyi *et al*., 2016a-d; Omotosho *et al*., 2016; Foo *et al*., 2010; Umoren *et al*., 2007). Based on $R_{Lg}$ values from Table 2 the adsorption is favourable. From the adsorption studies conducted the Langmuir adsorption isotherm explains the metal-inhibitor interaction mechanism in the corrosion system. It therefore presumes that there are no interactions between the inhibitor molecules adsorbed on the metal surface.

Furthermore, in a bid to evaluate the adsorption mechanism of $K_2CrO_4$, the Gibbs free energy (Δg adsorption°) of adsorption was deduced by the expression in Eq. 7 (Okeniyi, 2016; Umoren *et al*., 2007):

$$\Delta G^{\circ}_{adsorption} = -2.303RT\text{Log}\left(55.5K_{Lg}\right) \quad (7)$$

R and T are the universal gas constant (8.314 kJ/mol•K) and ambient temperature (303 K), respectively. By substituting the $K_{lg}$ value from Table 2 into the Gibbs free energy of adsorption equation a value of -9.8 kJ/mol is arrived at. This negative value indicates a spontaneous adsorption process for the inhibitor (Fig. 5).

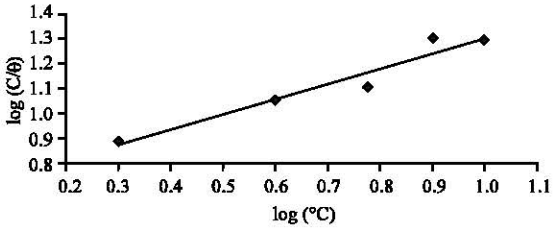


Fig. 5: Experimental data fit to the Langmuir adsorption isotherm for potassium chromate on the mild steel surface at a room temperature of 30°C

## CONCLUSION

This research focused on mild steel corrosion in 0.5 M $H_2SO_4$ solution with and without varying concentration of $K_2CrO_4$ at ambient temperature of 30°C and steady state condition using gravimetric and Tafel polarization measurements. The under-listed are the conclusions from the study: The trend of the corrosion rate in terms of reducing corrosion rate is 2<4<6<8<10 g/L.

The inhibitor efficiency of $K_2CrO_4$ on the corrosion of mild steel in 0.5 M $H_2SO_4$ solution increases with increasing inhibitor concentration. The Tafel polarization curve shows that the potassium chromate inhibitor is a mixed but predominantly anodic-type inhibitor. This infers the inhibitor activity influences activity at the cathodic sites. The $K_2CrO_4$ adsorption on the metal obeys the Langmuir adsorption isotherm. It is also a spontaneous process because of the negative value of Δg° adsorption obtained. The negative sub -20 kJ/mol value show predominance of physical adsorption process of the chromate inhibitor on the steel surface. Based on separation factor $R_{Lg}$, obtained the adsorption of the inhibitor on the metal surface is favourable.

## ACKNOWLEDGEMENTS

The researchers wish to acknowledge the laboratory contributions of Engr. Badmus of the Environmental and Water Resources Laboratory. The financial and equipment support of Covenant University Management towards the actualization of the research is also appreciated.

## REFERENCES

ASTM D2688-94 R99, 2005. Standard test methods for corrosivity of water in the absence of heat transfer (weight loss methods). ASTM International, West Conshohocken, PA., USA.

ASTM., 2005. Standard practice for preparing, cleaning and evaluating corrosion test specimens. ASTM G 1-03, ASTM International, West Conshohocken, PA.

Canmet, S.P., 2008. Electrochemical Polarization Techniques for Corrosion Monitoring. In: Techniques for Corrosion Monitoring, Yang, L. (Ed.). Elsevier, Cambridge, ISBN: 9781845694050, pp: 49-85.

Deberry, D.W., G.R. Peyton and W.S. Clark, 1984. Evaluation of corrosion inhibitors in $SO_2$ scrubber solutions. Corrosion, 40: 250-256.

Eddy, N.O., H. Momoh-Yahaya and E.E. Oguzie, 2015. Theoretical and experimental studies on the corrosion inhibition potentials of some purines for aluminum in 0.1 M HCl. J. Adv. Res., 6: 203-217.

Finsgar, M. and J. Jackson, 2014. Application of corrosion inhibitors for steels in acidic media for the oil and gas industry: A review. Corrosion Sci., 86: 17-41.

Foo, K.Y. and B.H. Hameed, 2010. Insights into the modeling of adsorption isotherm systems. Chem. Eng. J., 156: 2-10.

Karthik, G. and M. Sundaravadivelu, 2013. Inhibition of mild steel corrosion in sulphuric acid using esomeprazole and the effect of iodide ion addition. ISRN Electrochem. 10.1155/2013/403542

Karthikaiselvi, R. and S. Subhashini, 2014. Study of adsorption properties and inhibition of mild steel corrosion in hydrochloric acid media by water soluble composite poly (vinyl alcohol-omethoxy aniline). J. Assoc. Arab Univ. Basic Appl. Sci., 16: 74-82.

Oguzie, E.E., G.N. Onuoha and A.I. Onuchukwu, 2005. Inhibitory mechanism of mild steel corrosion in 2 M sulphuric acid solution by methylene blue dye. Mater. Chem. Phys., 89: 305-311.

Okeniyi, J.O., 2016. $C_{10}H_{18}N_2Na_2O_{10}$ inhibition and adsorption mechanism on concrete steel-reinforcement corrosion in corrosive environments. J. Assoc. Arab Univ. Basic Appl. Sci., 20: 39-48.

Okeniyi, J.O., C.A. Loto and A.P.I. Popoola, 2014a. *Morinda lucida* effects on steel-reinforced concrete in 3.5% NaCl: Implications for corrosion-protection of wind-energy structures in saline/marine environments. Energy Procedia, 50: 421-428.

Okeniyi, J.O., C.A. Loto and A.P.I. Popoola, 2014b. *Rhizophora mangle* L. effects on steel-reinforced concrete in 0.5 M $H_2SO_4$: Implications for corrosion-degradation of wind-energy structures in industrial environments. Energy Procedia, 50: 429-436.

Okeniyi, J.O., C.A. Loto and A.P.I. Popoola, 2014c. Corrosion inhibition performance of *Rhizophora mangle* L. bark-extract on concrete steel-reinforcement in industrial-microbial simulating-environment. Intl. J. Electrochem. Sci., 9: 4205-4216.

Okeniyi, J.O., C.A. Loto and A.P.I. Popoola, 2015a. Corrosion inhibition of concrete steel-reinforcement in saline/marine simulating-environment by *Rhizophora mangle* L. Solid State Phenomena, 227: 185-189.

Okeniyi, J.O., C.A. Loto and A.P.I. Popoola, 2015b. Evaluation and analyses of *Rhizophora mangle* L. leaf-extract corrosion-mechanism on reinforcing steel in concrete immersed in industrial/microbial simulating-environment. J. Applied Sci., 15: 1083-1092.

Okeniyi, J.O., C.A. Loto and A.P.I. Popoola, 2015c. Investigating the corrosion mechanism of *Morinda lucida* leaf extract admixtures on concrete steel rebar in saline-marine simulating environment. Intl. J. Electrochem. Sci., 10: 9893-9906.

Okeniyi, J.O., C.A. Loto and A.P.P. Idowu, 2014d. Inhibition of steel-rebar corrosion in industrial/microbial simulating-environment by *Morinda Lucida*. Solid State Phenom., 227: 281-285.

Okeniyi, J.O., I.O. Oladele, O.M. Omoniyi, C.A. Loto and A.P.I. Popoola, 2015d. Inhibition and compressive-strength performance of $Na_2Cr_2O_7$ and $C_{10}H_{14}N_2Na_2O_8 \bullet 2H_2O$ in steel-reinforced concrete in corrosive environments. Can. J. Civil Eng., 42: 408-416.

Okeniyi, J.O., O.A. Omotosho, C.A. Loto and A.P.I. Popoola, 2017. Anticorrosion and adsorption mechanism of *Rhizophora mangle* l. leaf-extract on steel-reinforcement in 3.5% NaCl-immersed concrete. Proceedings of the 3rd Congress on Pan American Materials, February 10, 2017, Springer, Cham, Switzerland, ISBN:978-3-319-52131-2, pp: 167-178.

Okeniyi, J.O., O.A. Omotosho, E.T. Okeniyi and A.S. Ogbiye, 2016. Anticorrosion Performance of Solanum Aethiopicum on Steel-Reinforcement in Concrete Immersed in Industrial Microbial Simulating-Environment. In: TMS 2016 145th Annual Meeting and Exhibition, Annual Meeting Supplemental Proceedings, the Minerals, Metals and Materials Society (Eds.). Springer, Berlin, Germany, ISBN:978-3-319-48624-6,pp: 409-41610.1007/978-3-319-48254-5.

Okeniyi, J.O., O.A. Omotosho, O.O. Ajayi and C.A. Loto, 2014. Effect of potassium-chromate and sodium-nitrite on concrete steel-rebar degradation in sulphate and saline media. Construct. Build. Mater., 50: 448-456.

Okeniyi, J.O., O.A. Omotosho, O.O. Ajayi, O.O. James and C.A. Loto, 2012. Modelling the performance of sodium nitrite and aniline as inhibitors in the corrosion of steel-reinforced concrete. Asian J. Applied Sci., 5: 132-143.

Okonji, P.O., R.E. Okonji and J.U. Odi, 2015. Effect of inhibitors on the corrosion behaviour of cold-rolled mild steel. Int. J. Scient. Res. Eng. Trends, 1: 5-8.

Omotosho, O.A., C.A. Loto, O.O. Ajayi, J.O. Okeniyi and A.P.I. Popoola, 2014. Investigating potassium chromate and aniline effect on concrete steel rebar degradation in saline and sulphate media. Int. J. Electrochem. Sci., 9: 2171-2185.

Omotosho, O.A., J.O. Okeniyi, A.B. Oni, T.O. Makinwa and O.B. Ajibola *et al*., 2016b. Inhibition and mechanism of Terminalia catappa on mild-steel corrosion in sulphuric-acid environment. Prog. Ind. Ecol. Intl. J., 10: 398-413.

Omotosho, O.A., J.O. Okeniyi, C.A. Loto, A.P.I. Popoola and C.E. Obi *et al*., 2016a. Performance of *Terminalia catappa* on mild steel corrosion in HCl medium. AIP. Conf. Proc., 1758: 030027-030027.

Omotosho, O.A., J.O. Okeniyi, C.A. Loto, A.P.I. Popoola and E.O.J. Fademi *et al*., 2017a. $C_6H_5NH_2$ effect on the corrosion inhibition of aluminium in 0.5M HCl. AIP Publishing, 1814: 010001-1-010001-2.

Omotosho, O.A., J.O. Okeniyi, C.A. Loto, A.P.I. Popoola and O.B. Ajibola *et al*., 2017b. Cassia Fistula Leaf-Extract Effect on Corrosion-Inhibition of Stainless-Steel in 0.5M HCl. In: Proceedings of the 3rd Pan American Materials Congress, Meyers, M.A., H.A.C. Benavides, S.P. Bruhl, H.A. Colorado and E. Dalgaard, (Eds.). Springer, Berlin, Germany, ISBN:978-3-319-52131-2, pp: 179-189.

Omotosho, O.A., J.O. Okeniyi, E.I. Obi, O.O. Sonoiki and S.I. Oladipupo *et al*., 2016c. Inhibition of Stainless Steel Corrosion in 0.5 M H2SO4 in the Presence of C6H5NH2. In: TMS 2016 145th Annual Meeting and Exhibition, Annual Meeting Supplemental Proceedings, The Minerals, Metals and Materials Society (Eds.). Springer, Berlin, Germany, ISBN:978-3-319-48624-6, pp: 465-472.

Omotosho, O.A., J.O. Okeniyi, O.O. Ajayi and C.A. Loto, 2012. Effect of synergies of $K_2Cr_2O_7$, $K_2CrO_4$, $NaNO_2$ and aniline inhibitors on the corrosion potential response of steel reinforced concrete in saline medium. Int. J. Environ. Sci., 2: 2346-2359.

Omotosho, O.A., O.O. Ajayi, O.S. Fayomi and V.O. Ifepe, 2011. Assessing the deterioration behaviour of mild steel in 2 M sulphuric acid using Bambusa glauscescens. Intl. J. Appl. Eng. Res. Dindigul, 2: 406-418.

Onuchukwu, A.I., 1988. Corrosion inhibition of aluminum in alkaline medium. I: Influence of hard bases. Mater. Chem. Phys., 20: 323-332.

Rani, B.E.A. and B.B.J. Basu, 2012. Green inhibitors for corrosion protection of metals and alloys: An overview. Int. J. Corrosion. 10.1155/2012/380217

Umoren, S.A., O. Ogbobe, P.C. Okafor and E.E. Ebenso, 2007. Polyethylene glycol and polyvinyl alcohol as corrosion inhibitors for aluminium in acidic medium. J. Applied Polym. Sci., 105: 3363-3370.

Yadav, J.K., B. Maiti and M.A. Quraishi, 2010. Electrochemical and quantum chemical studies of 3,4-dihydropyrimidin-2(1H)-ones as corrosion inhibitors for mild steel in hydrochloric acid solution. Corrosion Sci., 52: 3586-3598.